Peer-reviewed version available at *Energies* **2019**, *12*, 2253; doi:10.3390/en12122253

Article

A Generalized and Mode-adaptive Approach to the Power Flow Analysis of the Isolated Hybrid AC/DC Microgrids

Yu Xiao[1], Chunguang Ren[1], Xiaoqing Han[1],*,Peng Wang[2]

[1] College of electrical and power engineering, Taiyuan University of Technology, Taiyuan, China; 47922675@qq.com (Y.X.) ; renchunguang55@163.com (C.R.)

[2] Nanyang Technological University, Singapore 639798, Singapore; epwang@ntu.edu.sg (P.W.)

* Correspondence: hanxiaoqing@tyut.edu.cn: Tel.:+86-0351-6010031

Received: 5 May 2019

Abstract: HybridAC/DC microgrids(HMG) are emerging as an attracting method for integrating the AC/DC distributed energy resources(DERs) with the features of high-performance and low-cost. In the isolated hybrid AC/DC microgrid (IHMG),the key problem is how to balance the power variation and regulate the voltage and frequency. Various energy storage systems (ESS)and interlinking converter (IC) technologies are viable for this application. The present study proposes a novel unified power flow model to evaluate and compare the abilities of the ESS with different connection topologies and ICs with different control approaches to maintain the voltage and frequency stability of the IHMG. In order to investigate the performance of the proposed scheme, five operation modes of the IHMG are defined and explained. The classification is based on the connection topologies and control modes of the ESS/IC in the IHMG. Then, a set of generic PF equations are derived. Moreover, three binary matrices are applied in the construction of the unified power equations. These matrices are used for describing the running state of the IHMG. Finally, in order to verify the proposed scheme, it is applied to several case studies of the IHMG. The operation characteristics of multi-DC subgrids IHMG in different modes, particularly when an external disturbance occurs, are investigated.

Keywords: hierarchical control; AC-DC hybrid microgrids; primary control; ESS; interlinking converter; power flow analysis

---

1. **Introduction**

In the renewable power generation systems, new features, such as the increment of the DC sources and loads and rapid developments in DC energy storage systems (ESSs)are emerging. This is more pronounced at the distribution level. In order to satisfy various operational requirements, Hybrid AC/DC microgrid (HMG) is introduced. It should be indicated that the HMG projects are widely adopted worldwide [1-3].Fig 1 shows a typical topology of the HMG and indicates that the HMG is composed of an AC and a DC network. Each network contains distributed generations (DGs), ESSs and loads. Moreover, an interlinking converter (IC) links the AC and DC microgrids together.

Compared to the conventional AC or DC microgrids, the isolated hybrid AC/DC microgrid (IHMG) reduces the equipment investment and the energy loss in the power conversion process by connecting sources and loads to the AC and DC buses with low power consumption for the

Peer-reviewed version available at Energies 2019, 12, 2253; doi:10.3390/en12122253

conversion. It is anticipated that the IHMGs will be the most promising microgrid structures in the near future [1].

There are two operating modes for the HMG, called the grid-tied mode and the isolated mode. Reviewing the literature shows that the latter mode has recently attracted significant attention because of its desirable characteristics, including the high availability of the electricity, profitability for consumers and electrification potentials for remote isolated small communities. The construction of isolated microgrids has evolved dramatically so far, to incorporate DC and hybrid AC/DC systems that can adapt to high penetration of DC-based DGs and loads [3].

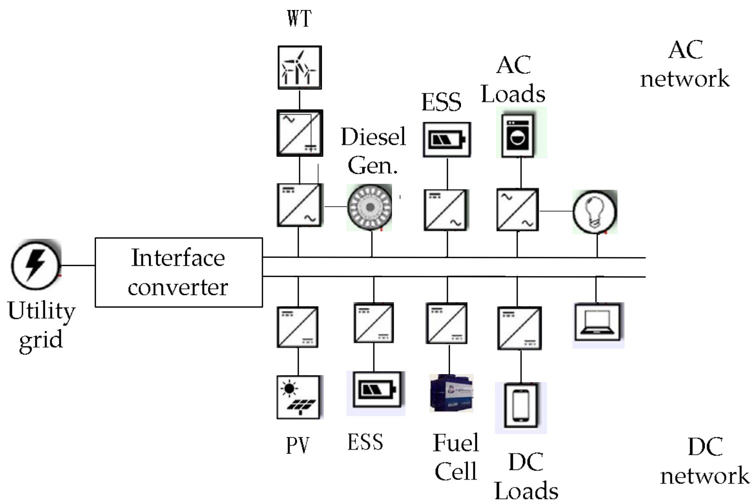

Figure 1. Layout of the AC/DC hybrid microgrid (HMG).

Extensive research has been conducted worldwide on the isolated HMG (IHMG). The power-flow (PF) analysis significantly contributes to the design, expansion planning and optimal operation of the HMG [9]. The power flow analysis indicates that the IHMG have specific characteristics that significantly differ from those of the conventional power grids [4,5].It was found that in the isolated mode, the frequency of the AC subgrid in the IHMG is no longer fixed, but changes frequently within a range due to uncertainty of primary resources, load and intra-day market factors. On the other hand, because of the development and wide applications of the droop control technology in the IHMG, the new type-droop bus is emerging. Therefore, the conventional methods for the node voltage modeling will be no longer suitable for IHMG applications. Moreover, the control strategies that are adopted by most authors in the isolated HMG are based on the hierarchical structure, which has detailed in the section. Union for the co-ordination of transmission of electricity (UCTE) and continental Europe raised the concept of hierarchical control. There are three main control levels, including the global/tertiary, microgrid/secondary and the local/primary control methods in this approach [6]. Unlike the secondary and tertiary controllers, which are generally based on similar controllers used in the systems, the primary control should be designed specifically for the application in the IHMG [6]. Therefore, multiple running scenarios with different frequency/voltage operation characteristics can be identified according to different primary control strategies. However, reviewing the literature shows that few studies for the IHMG power flow analysis are performed to date for the diversification of the operational modes of the IHMG.

Researchers considered the unique operational characteristics of the IHMG, such as the unavailability of a slack bus, droop controllability of the interfaced converter of the distributed generation and the bidirectional power flow between neighboring subgrids to modify the conventional methods and develop new approaches for analyzing the power flow [9]-[19].

Eajal, Mohamed and El-Saadany [11] used a set of linear and nonlinear equations and proposed a detailed modeling approach for the isolated IHMG. Meanwhile, they applied a united,

Peer-reviewed version available at Energies 2019, 12, 2253; doi:10.3390/en12122253

globally convergent and trust-region Newtonian method to solve the equations. Based on the results of the power flow analysis, they pointed out that the major difficulties of the IHMG originate from the equal power sharing. Aprilia et al. [9] proposed the coupling of the AC frequency and the DC voltage in the IHMG and discussed the modeling method. They performed variety of calculations and investigated the operational characteristics of the HMG with several DC subgrids. Hamad, Azzouz and EI-Saadany [12] adopted the Newton Raphson (NR) method to handle the unique features of the IHMG with lower computational time. Aprilia, Meng, Hosani, Zeineldin and Dong[16] proposedthe united power flow algorithm in emphasis on the incorporation of the IC droop control through the coupling of the normalized AC frequency and the DC voltage. Li, Chaudhary and Saadany [13] implemented the virtual impedance into the PF mathematical model. However, the model separately used AC or DC microgrids. Ahmed, Eltantawy, and Salama [15] proposed a general PF mode that can be applicable to the PF analysis of the AC-DC hybrid distribution network with varied mixed configurations of lines and buses. However, he only focused on the network structure and ignored the influence of the component control method on different network structures.

Studies show that there are two general methods, including the unified and sequential methods, for the power flow calculation of the AC/DC hybrid network [21]-[23]. Moreover, multiple iterative loops should be solved sequentially and separately in the sequential method, which leads to the increase of computational time and complexity [22]. It should be indicated that this problem is resolved in the unified algorithm [23].

In the present study, a unified PF model is introduced to compare various practice steady operation states, based on the general consideration of the influence of existing control strategies on the IHMG. The proposed model is unique from the formulation point of view. Various realistic voltage and frequency control scenarios are considered in the IHMG to unify AC/DC PF equations. The performance of the proposed method will be analyzed in independent test cases for the AC and DC microgrids. The developed model employs three binary matrices to describe the configuration and operational mode of the IHMG. The generic AC and DC power equations are constructed. Moreover, the proposed model is used for solving the PF problem. In order to evaluate the effectiveness and the accuracy of the proposed mode, the PF results are compared with those obtained from the MATLAB software. The unified PF model proposed in this paper can be used for grid operators to fully understand the characteristic of different operationalmodes, which have been formed by different quasi-steady-state control strategies in the IHMG. This is more pronounced when the standardization of the supervisory control remains unclear.

The remainder of the presents study is organized as follows: Section 2 provides a brief overview of the hierarchical control for the application of the IHMG and emphatically presents the primary control adopted by grid units of the IHMG. The definitions of the five operational scenario-based control strategies are discussed in details in section 3. Moreover, section 4 deduces the formulation of the proposed PF model, including the unified AC-DC power equations, in details. Furthermore, the case studies for various operation modes in the IHMG with different configuration and the validation of the proposed PF model are described in section 4. Finally, section 5 presents the conclusion of the present study.

2. Primary Control in The Hierarchical Controlled AC/DCIHMG

2.1. Hierarchical Control Level

The ability of supporting the AC frequency and DC voltage are the essential features for the IHMGs, when they are disconnected from the main power grid. In fact, there is an obligation for

Preprints (www.preprints.org) | NOT PEER-REVIEWED | Posted: 6 May 2019 doi:10.20944/preprints201905.0067.v1

Peer-reviewed version available at Energies 2019, 12, 2253; doi:10.3390/en12122253

complex control architectures to support the AC frequency and DC voltage. A structured approach using the centralized or distributed control is called the multilevel-hierarchical control [5-8].This structure is extensively applied in low-speed communications. In general, three levels are defined in the hierarchical control strategy:

1. Level 1(primary control): The control object of this level achieves voltage/frequency control for interface devices of the distributed energy resources DER. Moreover, the power sharing and optimal power management of resources can be obtained.
2. Level 2(secondary control): The control level utilizes the low speed communication network to compensate the voltage and frequency deviations caused by the primary control level.
3. Level 3(tertiary control): there is a positive response in this control level for external dispatching instructions to maintain the effectiveness, economy and reliability of the system.

2.2. The Primary Control of The DERs in The IHMG

As the most critical levels in the hierarchical management, there are two distinguished types of primary control levels, namely the grid-following and grid-forming controls [5-8]. The purpose of the grid-following control is to extract as much power as possible from the renewable energy resource. For instance, the maximum power point tracking (MPPT) mode in the wind turbine and photovoltaic systems and the operation in the rated power in diesel/biomass generators are practical applications of the grid-following control [24-25].Moreover, the inverter-based renewable DGs have the capability of reactive power control by means of their inverters. It should be indicated that PV systems and wind turbines are required to participate in some grid codes to provide reactive power control of the power system[26].The connected buses in the aforementioned resources are usually modeled as PQ buses in the power flow analysis[13].

The grid-forming control, which mostly acts in intentional or non-intentional islanding mode, provides stability of the voltage and frequency. Furthermore, these control strategies falls into two categories based on the need or non-need of communication networks between devices[3].The former category includes master/slave, central or concentrated control, instantaneous current sharing or circular chain approaches. While the latter one mainly includes the droop-based control andthe virtual impedance. Usually, energy storage device or DGs based on the droop control techniques operatein the grid-forming mode[26,29]. The ω-P droop of an AC type ESS connected in n^{th} bus can be calculated by equation (1).

$$P_{SD,n} = \begin{cases} -P^{ch}_{SD,n,max}\,, & \text{if } \omega > \omega^{ch}_{max}\,, \\ \dfrac{1}{k_{spn}}(\omega_0 - \omega)\,, & \text{if } \omega^{dis}_{max} \le \omega \le \omega^{ch}_{max}\,, \\ P^{dis}_{SD,n,max}\,, & \text{if } \omega < \omega^{dis}_{max}\,, \end{cases} \tag{1}$$

Where the subscripts SD, n and sp denote the ESS units with the droop control, n^{th}AC bus and the active power droop gain, respectively. Moreover, $P^{ch}_{SD,an,max}$ and $P^{dis}_{SD,an,max}$ are the AC type ESS maximum active power charging and discharging rates, respectively. Furthermore, ω^{ch}_{max} and ω^{dis}_{max}denote the frequency at which the ESS starts to charge and discharge at its maximum charging or discharging rates, respectively. Finally, $k_{spn}$is defined as the following:

$$k_{spn} = \frac{\omega_{max}^{ch} - \omega_{max}^{dis}}{P_{SD,an,max}^{ch} + P_{SD,an,max}^{dis}} \quad (2)$$

the ω-P and V-Q droop of an AC type DG connects to the n^{th} bus, while the V-P droop of an DC type DG connects to the m^{th} bus.They are described by equations (3) to (5), respectively.

$$P_{GD,n} = \frac{1}{k_{pn}}(\omega^0 - \omega) \quad (3)$$

$$Q_{GD,n} = \frac{1}{k_{qn}}(|V_{GD,n,0}| - |V_{GD,n}|) \quad (4)$$

$$P_{GD,m} = \frac{1}{k_{pm}}(V_{GD,dm,0} - V_{GD,dm}) \quad (5)$$

Where the subscripts GD, n and m present the AC-type DG with the droop control, n^{th} AC bus and m^{th} DC bus, respectively.Moreover, $P_{GD,n}$ and $Q_{GD,n}$ denote the AC-type active and reactive output power, respectively and $P_{GD,m}$ is the DC-type active output power. Furthermore, k_{pn},k_{qn} and k_{pm} are the active and reactive droop gain of an AC-type DG and the active droop gain of a DC-type DG, respectively. It should be indicated that k_{pn} , k_{qn} and k_{pm} are defined by (6)-(8), respectively.

$$k_{pn} = \frac{\omega_{max} - \omega_{min}}{P_{GD,n,max}} \quad (6)$$

$$k_{qn} = \frac{|V_{GD,n}|_{max} - |V_{GD,n}|_{min}}{Q_{GD,n,max}} \quad (7)$$

$$k_{pm} = \frac{V_{GD,m,max} - V_{GD,m,min}}{P_{GD,m,max}} \quad (8)$$

Usually, these units are modeled as droop buses during the power flow analysis [10-12].The use of such quasi-steady control characteristics can significantly increase the complexity of the power flow.

2.3.The Primary Control of The IC in The IHMG

As a key element of the IHMG, the IC can achieve the following functions:

1. IC can be a slack bus for the AC subgrid compensating power mismatch in the AC subgrid in the weak systems, while the DC subgrid has a higher power surplus [12]. In this case, the IC can operate in the grid-forming mode to perform the frequency and voltage control of the AC subgrid.
2. IC can be a slack bus for the DC subgridwith lower power surplus capacity than that of the AC subgrid. Moreover, IC can perform the voltage control of the DC subgrid as a grid-forming unit in the DC subgrid.
3. In order to achieve the equal loadings of subgrids, both subgrids of the IHMG should have similar power, when the IC controls the transfer of the active power between the neighboring AC and DC subgrids. Moreover, in order to adapt the active power transfer between the two subgrids, IC measures the AC frequency and DC voltage and equalizes them by normalizing. The corresponding control strategies are as the following:

$$\widehat{\omega} = \frac{\omega - 0.5(\omega_{max} + \omega_{min})}{0.5(\omega_{max} - \omega_{min})} \quad (9)$$

Peer-reviewed version available at Energies 2019, 12, 2253; doi:10.3390/en12122253

$$\widehat{V}_{dc} = \frac{V_{dc} - 0.5(V_{c,dc}^{max} + V_{c,dc}^{min})}{0.5(V_{c,dc}^{max} - V_{c,dc}^{min})} \tag{10}$$

$$\Delta e = \widehat{\omega} - \widehat{V}_{dc} \tag{11}$$

$$P_C = -\frac{1}{k_{IC}}\Delta e \tag{12}$$

Where P_C is the power transferred from the DC to the AC subgrids through the IC in the IHMG.

Since the flow of the active power is from the DC to AC side, the IC can also support the reactive power at the AC side [30,31]. The injected reactive power of the IC to the AC network through the j[th] AC terminal is expressed as:

$$Q_c = \begin{cases} \min\left(\frac{1}{k_{qj}}(|V_{ac,j,0}| - |V_{ac,j}|), Q_{lim,j}\right) & \text{if } P_{c,ac,j} > 0 \\ 0 & \text{otherwise} \end{cases} \tag{13}$$

$$Q_{lim,j} = \sqrt{(S_{lim,i})^2 - (P_{c,ac,j})^2} \tag{14}$$

Where $P_{c,ac}$ is the injected active power by the converter at the AC side and S_{lim} and Q_{lim} are the apparent and reactive power limits of the IC, respectively.

3. Definition of The Operating Modes in The AC/DC IHMG

3.1. Classification of The AC/DC IHMG Configurations

The structural characteristics of the AC/DC IHMG can be summarized as the following:

1. Disconnecting from the main network.

2. Connecting the AC and DC subgrids through bidirectional AC/DC interfacing converters(ICs) to fulfill the bidirectional power flow between subgrids.

3. Dividing the zones according to the DER type, such as RES, DG and ESS, and load type, such as AC or DC.

Based on the aforementioned classifications, the location of the adopted device for the grid-forming control is closely related to the operating characteristics of the system.

Studies [30，31]showed that the AC/DC storage systems (e.g. battery bank, super capacitor and flywheel) and the IC devices, which usually operate in the grid-forming mode, can maintain the voltage and frequency stability of the IHMG. This means that the power difference between the output power of the RES and that of time-variable loads is been modified by the output power of the ESS/IC. It should be indicated that loads may vary with time because of variety of parameters, including weather conditions, prediction error and so on. The droop control strategies are appliedfor the application of the AC or DC ESS in accordance with equation (1). The controlled IC in the constant AC voltage control can maintain the frequency stability in the AC subgrid.Moreover,it can maintain the voltage stability in the DC subgrids in the constant DC voltage control mode. Several network configurations can be found in the literature, which are distinguished by the location of the storage units.Fig 1 shows an HMG system as examples,where its configuration falls into three categories when disconnecting from utility grid as the following: 1)

Storages as grid-forming devices are located only in the AC subgrid. 2) Storagesarelocated only in the DCsubgrid. 3)Storages are locatedin both subgrids.

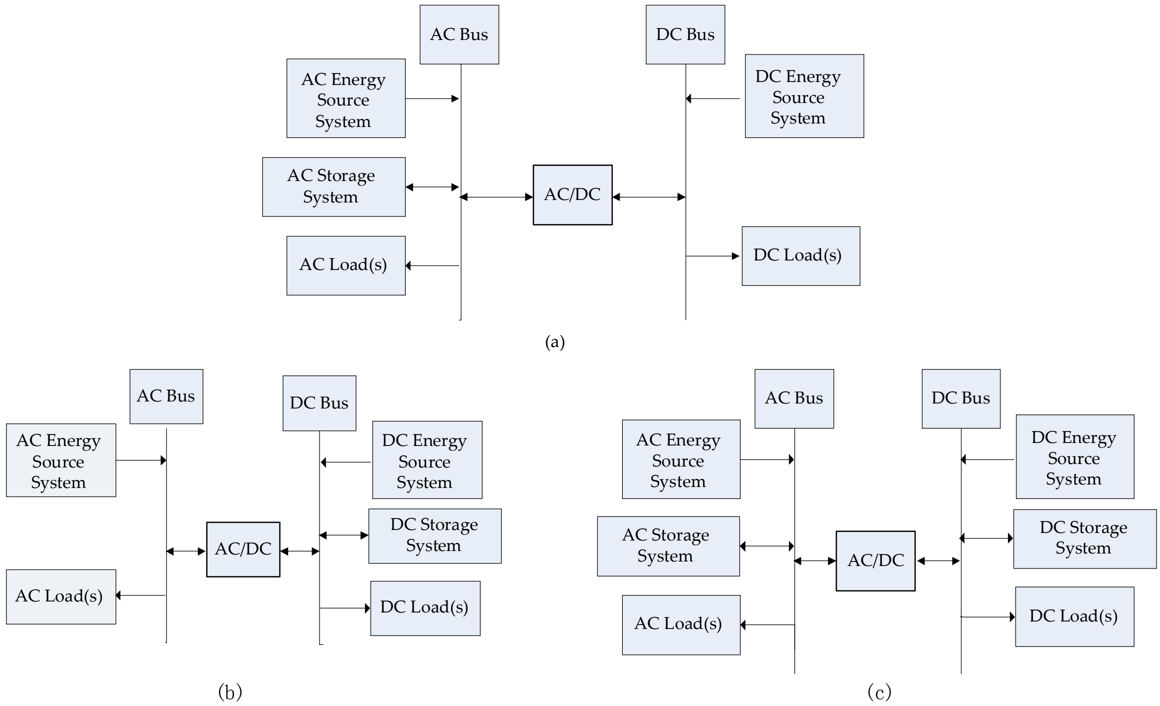

Figure 2. Classification of the configurations of the IHMG system: **(a)**Grid-forming units are in the AC subgrid, **(b)**Grid-forming units are in the DC subgrid and**(c)**Grid-forming units are in both AC and DC subgrids.

3.2. Primary Control Operating Modes

Based on the aforementioned three topological structures, the following five primary control operating modes are identified for the system configuration in accordance with Fig 1.

1. Single grid-forming unit in the AC network:

There is an ESS, which operates in the AC network as the grid-forming unit. Whereas, DGs of both subgrids operate in the grid-following mode. The frequency and voltage of the AC subgrid are sustained by the grid-forming unit and the voltage of the DC network is regulated with the IC between both networks. Moreover, the DC bus of the IC can operate as the DC slack bus of the DC subgrid.

2. Multiple grid-forming units in the AC network:

More than one storage system is actively involved as grid-forming units, in the control of the voltage and frequency of the AC network of the IHMG. An adequate power sharing strategies of grid-forming units is implemented for balancing the power variations of the IHMG. The method for power management of the DC network is similar to that of mode (1).

3. Single grid-forming unit in the DC network:

In the operating mode, the grid-forming unit and the DC energy storage are placed at the DC network. Moreover, the IC establishes the voltage and frequency in the AC network, so its AC bus operates as the AC slack bus of the AC subgrid. The operating principle is the same as that for mode (2).

4. Multiple grid-forming units in the DC network:

The power management is performed in the similar way as mode (2). The difference is these grid-forming units control the dc voltage of the dc network while being ensured an adequate power sharing between units. The IC established the frequency in the ac side.

Preprints (www.preprints.org) | NOT PEER-REVIEWED | Posted: 6 May 2019 doi:10.20944/preprints201905.0067.v1

Peer-reviewed version available at Energies 2019, 12, 2253; doi:10.3390/en12122253

5. multiple grid-forming units in both networks:

In the last operating mode, more than one grid-forming unit is placed at both networks. These AC/DC grid-forming units are placed in separate subgrids and can balance the power variations of the whole grid through the ICand transfer the active power between the neighboring two subgrids. The direction of the power flow always transforms into the subgrid with the worst power deficiency. Therefore, no special communication system is required.

Tables 1-3 present the corresponding electrical behavior of units in three main primary control operating modes in the islanded HMG.

Table 1. The electrical behavior of the main components of IHMG in mode 1

Unit type in mode 1	**Source type**	**Control type**	**Output impedance**	**PF model**
AC ESS or DG	Non-Ideal Voltage source	Droop[1]	Finite, nonzero	Droop
RES	Ideal current source	MPPT	0	PQ
IC	DC Ideal Voltage source	Constant DC Voltage control	0	DC constant V
DC ESS or DG	-	**-**	-	-

[1]See formula (1)-(6)

Table 2. The electrical behavior of the main components of IHMG in mode 3

Unit type in mode 3	**Source type**	**Control type**	**Output impedance**	**PF model**
AC ESS or DG	-	-	-	-
RES	Ideal current source	MPPT	0	PQ
IC	AC Ideal Voltage source	Constant AC Voltage control	0	AC constant V
DC ESS or DG	Non-Ideal Voltage source	Droop[2]	Finite, nonzero	Droop

[2]See formula (7)-(8)

Table 3.The electrical behavior of the main components of IHMG in mode 5

Unit type in mode 5	**Source type**	**Control type**	**Output impedance**	**PF model**
AC ESS or DG	Non-Ideal Voltage source	Droop[1]	Finite, nonzero	Droop

RES	Ideal current source	MPPT	0	PQ
IC	Non-Ideal Voltage source	Droop[3]	Finite, nonzero	Droop
DC ESS or DG	Non-Ideal Voltage source	Droop[2]	Finite, nonzero	Droop

[1]See formula (1)-(6);

[2]See formula(7)-(8);

[3]See formula(9)-(14).

4. Formulation of the unified PF model

4.1. DER Model

In AC/DC IHMGs, AC-type DERs can operate in three operation modes, including PQ, PV and the droop modes. Similarly, DC-type DERs can also operate in three modes, including the constant P, constant V and the droop modes. All mode are defined based on the primary control approach, adopted by the interface conversion of DERs.

In this section, some variables are defined as the following: $\mathrm{N_D}$ and $\mathrm{M_D}$ are the number of units in the grid-forming control in the AC subgrid (e.g. AC ESS/DGs in the AC droop control) and the DC subgrid (e.g. DC ESS/DGs in the DC droop control), respectively. Moreover, $\mathrm{N_R}$ and $\mathrm{M_R}$are the number of units in the grid-following control in the AC and DC subgrids, respectively. On the other hand, $\mathrm{N} = \mathrm{N_D} + \mathrm{N_R}$ and $\mathrm{M} = \mathrm{M_D} + \mathrm{M_R}$ are the total number of buses in the AC and DC subgrids, respectively. The corresponding quantities of various bus connected units are summarized in Table 4.

Table 4. The Variables for the buses of IHMG

Subgrid	**Bus type**	**Number of buses**	**Known quantity**	**Unkonwn quantity $x=[x_{AC},x_{DC}]$**	**Number of equations**
AC	PQ	N_R	P_n, Q_n	V_n, δ_n	$2N_R$
	Droop	N_D	-	P_n, Q_n, V_n, δ_n	$4N_D$
	Slack bus	1	V_n, δ_n	P_n, Q_n	-
DC	Const.P	M_R	P_m	V_m	M_R
	Droop	M_D	-	P_m, V_m	$2M_D$
	Const.V	$M-M_R-M_D$	V_m	P_m	$M-M_R-M_D$

4.2 Formulation of The Unified PF Model

In order to implement the PF model for any generic operational models in accordance with definitions discussed in section 3, the system configuration and parameters should be described in a matrix format. The following matrices are defined in this regards. It should be indicated that they are used as inputs for the LF model.

1. Unit-type vector W((N+M)×1); It describes the unit type (i.e. grid-following or grid forming) connected to the relevant bus in the AC/DC subgrid, as the following:

i) When W_i=1, the bus connects to the grid-forming unit.

ii) When W_i=0, the bus does not connect to the grid-following unit.

2. Judgment vector D((N+M)×1); It checks for the coexistence of grid-forming units in both AC and DC subgrids:

i) When D_i=1, the grid-forming unit is available in both AC and DC subgrids.

ii) When D_i=0, the grid-forming unit is only installed separately in the AC or DC subgrids.

3. Judgment vector U((N+M)×1); It checks for the existence of the grid-forming unit in each AC or DC subgrids:

i) When U_i=1, there are grid-forming units in the ACsubgrid.

ii) When U_i=0, there is not grid-forming unit in the AC subgrid;.

4. The AC admittance matrix Y(N×N);

$$Y_{nk}(\omega) = G_{nk}(\omega) + jB_{nk}(\omega) = \frac{1}{R_{nk}+j\omega L_{nk}}, \quad \mathrm{n,k} \in \mathrm{N} \tag{15}$$

5. DC conductance matrix $\mathrm{G^{dc}}(\mathrm{M} \times \mathrm{M})$; The element in the matrix reflects the value of the conductance of the DC line that connects two buses.

4.3 Power balance equations

Power balance equations are derived based on the configuration cases defined in section 3 and the configuration matrices(W, D and U). For a given set of elements of the above matrices, only one configuration is activated in the power equations at the same time. The elements of matrices reflect operating modes in the IHMG system and they are summarized in table 5.

Table 5. The values of U, D and W matrices, corresponding to operating modes of the IHMG.

Mode type	U_i	D_i	W_i
Mode 1	1	0	1
Mode 3	0	0	0
Mode 5	1	1	1

It should be indicated that when values of the matrix element are equal to those for the mode 1 but the number of corresponding nodes is greater than 1, the operating mode of the IHMG is identified as the mode 2. Similarly, when values of the matrix element are the same as those for the mode 3 but the number of corresponding nodes is greater than 1, the operating mode of the IHMG is identified as the mode 4.

The active and reactive power mismatch equations for thebuses of AC and DC subgridsof the IHMG system are expressed in equations (16) and (17), respectively.

$$F_{Pn}(\delta_n, |V_n|, f) = P_{ac,n}^{inj} = 0, \quad \forall\, \mathrm{n} \in \mathrm{N} \tag{15}$$

$$F_{Qn}(\delta_n, |V_n|, f) = Q_n^{inj} = 0, \forall \mathrm{n} \in \mathrm{N} \tag{16}$$

$$F_{Pm}(V_m) = P_{dc,m}^{inj} = 0, \forall\, \mathrm{m} \in \mathrm{M} \tag{17}$$

Moreover, $\mathrm{P_{ac,n}^{inj}}$, $\mathrm{Q_n^{inj}}$ and $\mathrm{P_{dc,m}^{inj}}$, are expressed in equations (18) to (20), respectively.

Preprints (www.preprints.org) | NOT PEER-REVIEWED | Posted: 6 May 2019 doi:10.20944/preprints201905.0067.v1

Peer-reviewed version available at Energies 2019, 12, 2253; doi:10.3390/en12122253

$$\begin{aligned}P_{ac,n}^{inj} = \widetilde{U}\big(P_{GR,n} + WP_{GD,n} - P_{L,n} - P_n - D\beta_n P_{cn}\big) \\ + U\big[\widetilde{D}\big(P_{GR,n} + WP_{GD,n} - P_{L,n} - P_n - D\beta_n P_{cn}\big) + D\big(P_{GR,n} \\ + WP_{GD,n} - P_{La,n} - P_n - D\beta_n P_{cn}\big)\big]\forall\, n = 1,2, \dots N\end{aligned} \tag{18}$$

$$Q_n^{inj} = Q_{GR,n} + Q_{GD,n} - Q_{Ln} - Q_n - \beta_n Q_{Cn} \tag{19}$$

$$\begin{aligned}P_{dc,m}^{inj} = U\big(P_{GR,m} + \widetilde{W}P_{GD,m} + DWP_{GD,m} - P_{L,m} - P_m + D\beta_m P_{cm}\big) \\ + \widetilde{U}\big[\widetilde{D}\big(P_{GR,m} + \widetilde{W}P_{GD,m} + DWP_{GD,m} - P_{L,m} - P_m \\ + D\beta_m P_{cm}\big) + D\big(P_{GR,m} + \widetilde{W}P_{GD,m} + DWP_{GD,m} - P_{L,m} \\ - P_m + D\beta_m P_{cm}\big)\big]\forall\, m = 1,2, \dots, M\end{aligned} \tag{20}$$

Where$\widetilde{U} = 1 - U$, $\widetilde{D} = 1 - D$and $\widetilde{W} = 1 - W$. Moreover, $P_{GD,n}$and$P_{GD,m}$are the active output power of the AC and DC ESS or DG units in the grid-forming control, respectively. Furthermore, $P_{GR,n}$ and $P_{GR,m}$are the active output power of the AC and DC RES units in the grid-following control, respectively. P_{cn}andP_{cm}indicate the active output power of the AC and DC terminal of the IC, when the IHMG system operate in mode 5. In this paper, the loss of the IC is ignored. Therefore, $P_{cn} = -P_{cm} = P_C$.On the other hand, $Q_{GR,n}$,$Q_{GD,n}$and Q_{Cn}denote the output reactive powers of the RES in the grid-following control, DG in the droop control and AC terminal of the IC, respectively.

$$P_n = |V_n| \sum_{k=1}^{N} |V_k|\,|Y_{nk}(\omega)| \cos(\delta_n - \delta_k - \theta_{nk}K(\omega)) \tag{21}$$

$$P_m = V_m \sum_{k=1}^{M} G_{mk} V_k \tag{22}$$

Where, P_n and $P_m$are the injected active power to the n^th^ AC bus and m^th^ DC bus, respectively. Moreover, $|Y_{nk}(\omega)|$and $\theta_{nk}(\omega)$ are the magnitude and phase angle of the nk^{th}entry in the AC bus admittance matrix, respectively. G^{mk}denotes the mk^{th}entry of the DC bus conductance matrix and$Q_n$is the injected reactive power to the m^th^ DC bus, which is expressed as:

$$Q_n = |V_n| \sum_{k=1}^{N} |V_k|\,|Y_{nk}(\omega)| \sin\big(\delta_n - \delta_k - \theta_{nk}(\omega)\big) \tag{23}$$

In order to summarize the aforementioned equations, the mathematical model of the whole system can be obtained as: $F(x)=\begin{cases}F_{AC}(x) = 0 \\ F_{DC}(x) = 0\end{cases}$. Where $F_{AC}(x)$ and $F_{DC}(x)$ are describing the mismatch equations of a general AC and DC bus and they are demonstrated as the following:

$$F_{AC}(x) \\ = \begin{cases} F_{Pn}\big(\delta_n, |V_n|, f, P_{GD,n}\big) = P_{ac,n}^{inj}\big(\delta_n, |V_n|, f, P_{GD,n}\big) n \epsilon N \\ F_{Qn}\big(\delta_n, |V_n|, f, Q_{GD,n}\big) = Q_n^{inj} = Q_{GR,n} + Q_{GD,n} - Q_{Ln} - Q_n - \beta_n Q_{Cn} n \epsilon N \\ F_{GD,Pn}\big(f, P_{GD,n}\big) = P_{GD,n} - \dfrac{1}{k_{pn}}(\omega_{n,0} - \omega) n \in N_D \\ F_{GD,Qn}\big(|V_{GD,n}|, Q_{GD,n}\big) = Q_{GD,n} - \dfrac{1}{k_{qn}}\big(|V_{GD,n,0}| - |V_{GD,n}|\big) n \in N_D \end{cases} \tag{24}$$

$$F_{DC}(x) = \begin{cases} F_{Pm}(V_m, P_{GD,m}) = P_{dc,m}^{inj}(V_m, P_{GD,m}) \qquad m \epsilon M \\ F_{GD,m}\big(P_{GD,m}, V_m\big) = P_{GD,m} - \dfrac{1}{k_{pm}}(V_{m,0} - V_m) m \in M_D \end{cases} \tag{25}$$

The Jacobian matrix at k^th^ iteration is defined by:

$$J\big(x^{(k)}\big) = \begin{bmatrix} J_{AC}^{(k)} & 0 \\ 0 & J_{DC}^{(k)} \end{bmatrix} \tag{26}$$

Peer-reviewed version available at Energies 2019, 12, 2253; doi:10.3390/en12122253

Where:

$$J_{AC}^{(k)}=\left.\frac{\partial F_{AC}}{\partial x_{AC}}\right|_{x_{AC}^{(k)}} \tag{27}$$

$$J_{DC}^{(k)}=\left.\frac{\partial F_{DC}}{\partial x_{DC}}\right|_{x_{DC}^{(k)}} \tag{28}$$

Variables x_{AC}, x_{DC} are detailed in Table 4.

4.3 Solution Procedure

In order to find the PF solution, a Newton TR dogleg method [31] is employed in the present work. It is a globally convergent iterative method and it is widely used for solving the highly nonlinear equations. The fsolve function of the MATLAB software is used to solve systems of equations by minimizing the sum of squares of the components. It should be indicated that the system of equation is solved,when the sum of squares is zero. The fsolve function has three algorithms: trust-region; trust region dogleg and levenberg-marquardt. The iterative solution procedure of the power flow can be best described by the flowchart in Fig. 3.

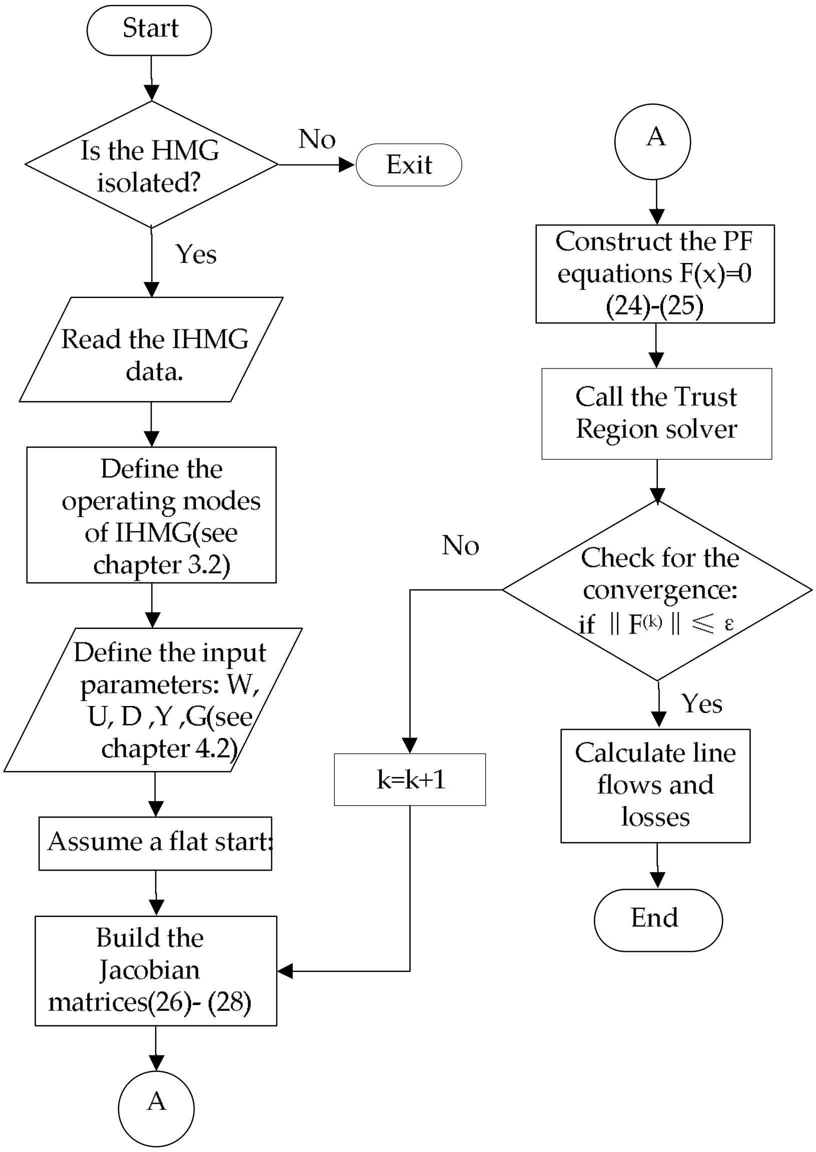

Figure 4. Flow chart of the proposed Mode-adaptive Powr flow algorithm of IHMG

5. **Cases Studies**

In this section, all operating modes of the islanded HMG are implemented in the studies cases. It should be indicated that considering the derived formulation of the problem, employment of different modes is highly facilitated.It is intended to investigate the performances of the proposed power flow methods and evaluate the quasi-steady-state behaviors of various primary control strategies.Therefore, the method is applied in fiveoperational modes after transient events.

5.1. Twelve-bus Test System

The accuracy of the proposed model is verified in comparison with the steady-state solution produced by the MATLAB software. The MATLAB is atime-domain software that utilizes differential equations and can accurately model power system components. Therefore, it can be used for validating LF algorithms [35,36].However, such software takes a huge amount of

Preprints (www.preprints.org) | NOT PEER-REVIEWED | Posted: 6 May 2019 doi:10.20944/preprints201905.0067.v1

Peer-reviewed version available at Energies 2019, 12, 2253; doi:10.3390/en12122253

computational time compared to the algebraic LF methods so that it should not be applied in the steady-state analysis [12].

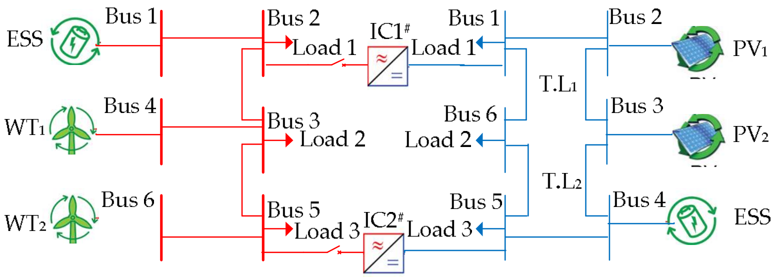

Fig 4.12-bus IHMG test system operating in mode 5

For testing the accuracy and effectiveness of the proposed LF model,it is applied on a 12-bus islanded AC/DC hybrid system, which is a modified test systems compared to the one use by Eajal, Mohamed and El-Saadany [11].Fig 4 shows the configuration of the test system. The system consists of radial and meshed topologies, wind turbine, photovoltaic system and a DS with droop control as grid-forming units in the both AC and DC subgrids. It should be indicated that both wind turbine and photovoltaic systems are equipped with MPPT control as grid-following units in the corresponding AC and DC subgrids. Fig 4 indicates that the system is running on mode 5. In this mode, the normalized droop control strategy adopted by the IC promotes the flexible bidirectional power flow between the AC and DC subgrids. This leads to high cooperation of DGs of the whole system to share the overall loading. However, conventional power flow algorithms fail to accurately simulate the characteristics of the introduced system [9-12]. In other words, thiscase study indicatesthe advantage of the proposed analysis method for the power flow over the conventional methods. The data related to generators, IC and corresponding bus classifications are presented in table 9-10.Moreover, the impedances of the network and the load connected to the related bus are summarized in table 11.The MVA and AC/DCKV base values are set to 3.0MW and 2.4/7KV, respectively. The results obtained from the proposed LF model and the steady-state solutions from the MATLAB software are listed in Tables 6-8.

It is found that the proposed method can solve the power flow in 1.5s, while the computational time of the MATLAB software is about 20s. Both the proposed algorithm and the MATLAB software are capable to reach steady at the frequency of 1.0021p.u. The maximum bus voltage magnitudes error and the maximum phase error are 0.06% and0.07%, respectively. These results indicate the accuracy of the proposed method.

Table 6. Test results of the voltage in the 12-bus IHMG system

Bus	**Bus type**	**Unified PF Results**		**MATLAB Results**	
		V_n **(p.u)**	θ_n **(p.u)**	V_n **(p.u)**	θ_n **(p.u)**
1(AC1)	Droop	0.9944	0.0337	0.9947	0.0330
2(AC1)	Droop(IC ac)	0.9928	0.0289	0.9932	0.0301

3(AC1)	PQ	0.9965	0.0234	0.9968	0.0256
4(AC1)	PQ(MPPT)	0.9957	0.0440	0.9960	0.0443
5(AC1)	Droop(IC ac)	0.9934	0.0956	0.9931	0.0900
6(AC1)	PQ(MPPT)	0.9994	0.0000	0.9997	0.0000
1^{dc} (DC2)	Droop(IC dc)	1.0086	—	1.0082	—
2^{dc} (DC2)	P	1.0012	—	1.0013	_—
3^{dc} (DC2)	P	0.9986	—	0.9981	—
4^{dc} (DC2)	Droop	0.9979	—	0.9972	—
5^{dc} (DC2)	Droop(IC dc)	1.0079	—	1.0076	—
6^{dc} (DC2)	R	0.9970	—	0.9969	—

[1]AC subgrid of the IHMG.

[2]DC subgrid of the IHMG.

Table 7. Test results of the output power of the DER in the 12-bus IHMG system

Bus	**Bus type**	**Unified PF Results**		**MATLAB Results**	
		$P_{DR,n}$ **(p.u.)**	$Q_{DR,n}$ **(p.u.)**	$P_{DR,n}$ **(p.u.)**	$Q_{DR,n}$ **(p.u.)**
1(AC[1])	Droop	-0.1325	—	-0.1361	—
4(AC[1])	PQ	0.2668	0.2013	0.2698	0.2000
6(AC[1])	Droop	0.5967	0.3034	0.5924	0.3001
2^{dc} (DC[2])	P	0.6098	—	0.6092	—
3^{dc} (DC[2])	Droop	0.0198	—	0.2001	—
4^{dc} (DC[2])	Droop	0.1998	—	0.1990	—

[1]AC subgrid of the IHMG;

[2] DC subgrid of the IHMG

Table 8. Test results of the transferred power by ICs in the 12-bus IHMG system

IC	Δe [1] (p.u)	V_{ac}^{2} (p.u)	V_{dc}^{3} (p.u)	P_c^{4} (p.u)	Q_c^{5} (p.u)
1#	0.038	0.9928	1.0086	-0.057	—
2#	0.052	0.9934	1.0079	-0.077	—

[1] The difference between the normalized AC frequency and DC voltage.

[2] The AC voltage amplitude of ICs.

[3] The DC voltage of ICs.

[4] The active power transferred by the IC.

[5] The reactive power transferred by the IC.

Table 9. Bus data for the 12-bus IHMG system

MG	Bus No.	Bus Type	$\lvert V_0 \rvert$ (p.u.)	DR Type	P_{DR}^{rated} MW	Q_{DR}^{rated} Mvar	ω_0 (p.u.)	m_p (p.u.)	n_p (p.u.)
AC	1	Droop	1.0	DS	0.8	0.6	1.0	0.0375	0.25
	2	Droop	1.0	--					
	3	Z	1.0	--					
	4	PQ	1.0	DG	0.48	0.36	1.0	0.0625	0.4167
	5	Droop	1.0	--					
	6	PQ	1.0	DG	1.8	1.35	1.0	0.0167	0.1111
DC	1	Droop	1.0						
	2	P	1.0	DG	1.92			0.0781	
	3	P	1.0	DG	0.48			0.3125	
	4	Droop	1.0	DS	0.6			0.25	
	5	R	1.0						
	6	Droop	1.0						

Table 10. The data for the IC of the 12-bus IHMG system

IC No.	AC Bus	DC Bus	P_{ic} (MW)	Q_{ic} (Mvar)	ω_0	$V_{dc,0}$ (p.u.)	γ_p	γ_q
1	2	1	3.0	2.25	1.0	1.0	1.0	0.0667

Peer-reviewed version available at *Energies* **2019**, *12*, 2253; doi:10.3390/en12122253

2	5	5	3.0	2.25	1.0	1.0	1.0	0.0667

Table 11. Line/Load data for the 12-bus IHMG system

MG	From	To	R(Ω)	X(Ω)	Load connected to From bus	
					P(MW)	Q(Mvar)
AC	1	2	0.02646	0.01323		
	2	3	0.04032	0.02016	0.4	0.3
	3	5	0.04032	0.02016	1.0	0.6
	5	6	0.02646	0.01323	0.8	0.6
	4	3	0.02646	0.01323		
DC	1	2	0.4340		0.6	
	2	3	0.2279			
	3	4	0.4100			
	4	5	0.4340			
	5	6	0.4100		1.4	
	6	1	0.2279		0.5	

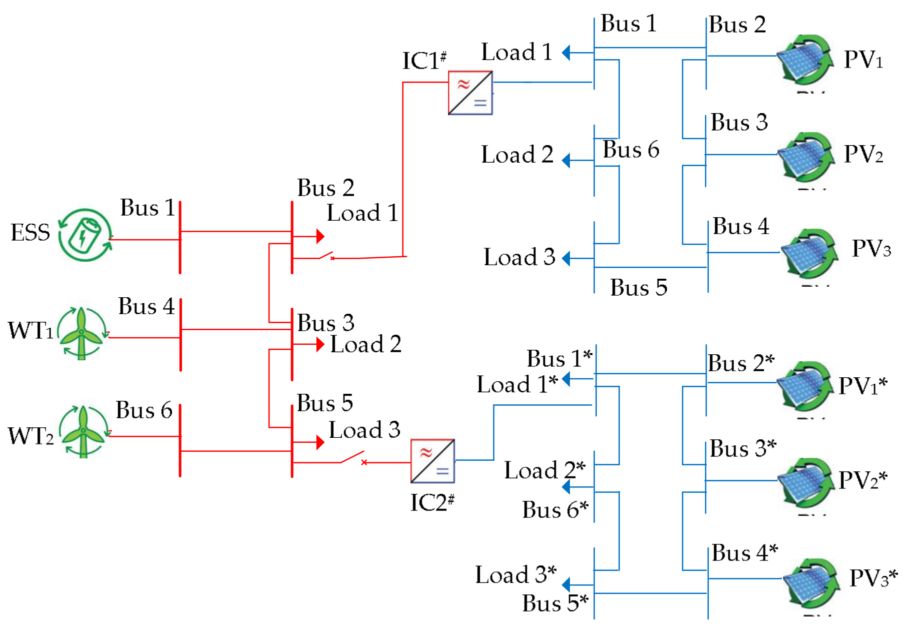

Fig 5. The multi-DC subgrids IHMG test system in the mode 1

5.2 Multi-DC subgridstest system

In this case, the mode 1, mode 2 and mode 5of the operation are compared and analyzed. The corresponding test systems are presented in Fig 5, Fig 6and Fig 7, respectively. They indicate that two identical DC subgrids with identical IC droop constants are connected to the 6-bus AC subgrid.

 doi:10.20944/preprints201905.0067.v1

Peer-reviewed version available at *Energies* **2019**, *12*, 2253; doi:10.3390/en12122253

Moreover, the DC subgrid 1 is connected to the AC bus 1, whereas the DCsubgrid 2 is connected to the AC bus 5.

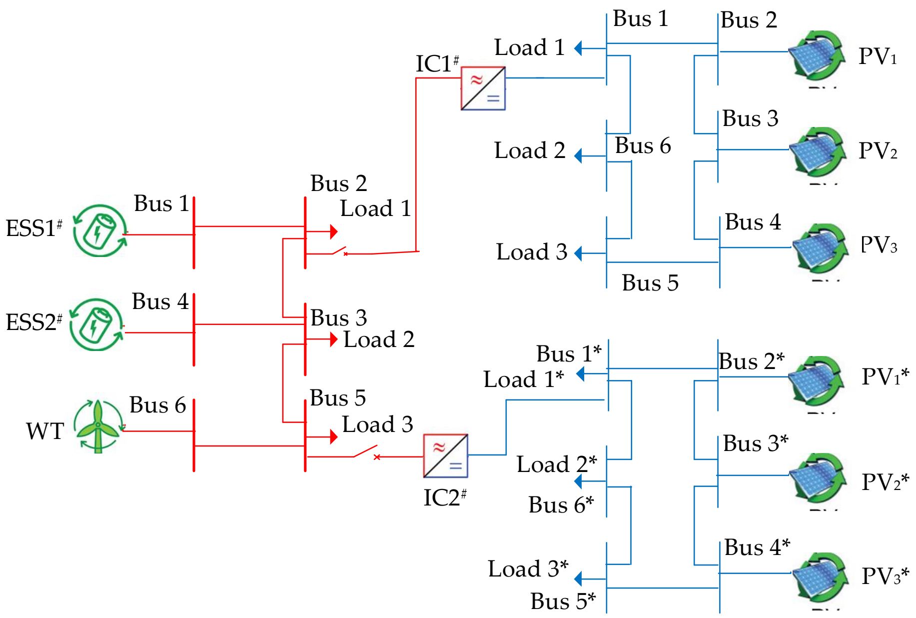

Fig 6. Multi-DC subgridsIHMG test system in the mode 2

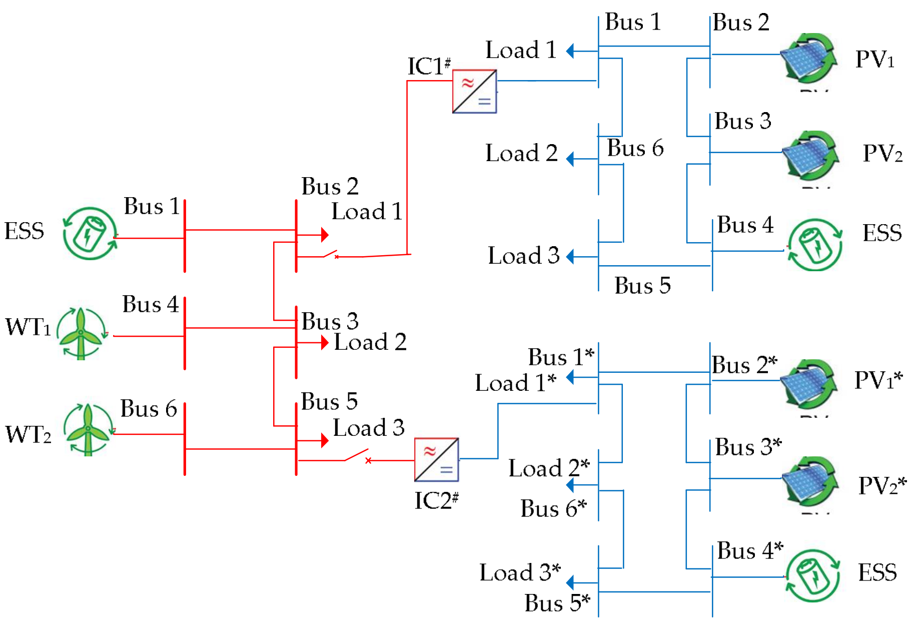

Fig 7. Multi-DC subgrids IHMG test system in the mode 5

All AC/DC subgrids are derived from the test system in case 1.In all three operational modes, the sum of ratings of power supplies and one of ESSs of the IHMG system are the same, while the deployment and the primary control approach adopted by each unit is distinct.Figs. 5 and 6 indicate that grid-forming ESSunit devices are only configured in the AC subgrid. .Moreover, it is observed that the total output power of the WT and the total ESS power rating of the AC subgridsare the same in Fig 5 and Fig 6. However,Fig 5illustrates that the configuration of the ESS is aggregated because only one unit is placed and the configuration of the WT is distributed- two same units placed.Fig. 6 shows that the topology of the mode 2 is opposite of that of the mode 1.It should be indicated that mode 5 of the operation is also tested in the multi-DC test system.

5.2.1. Algorithm Performance in The normal Potation of The Multi-DC Subgirds System

Fig 8 illustrates the DC bus voltages profile of the subgrid 1in different modes, where the subgrid 2 has an identical one.

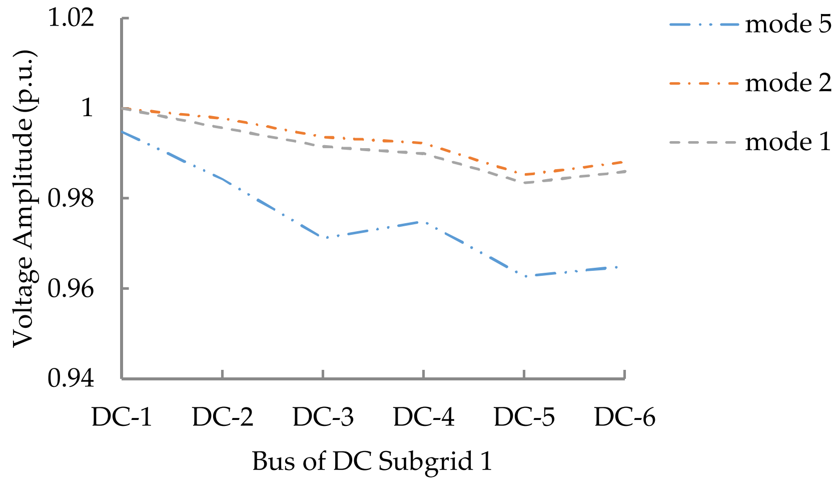

Fig 8. The DC bus voltage profiles of theDC subgrid 1

The present study intends to investigate the performance of the hierarchical structure, based on the centralized and distributed controls. Mode 1 and mode 2 belong to the former control, while the mode 5 belongs to the latter control. Fig 8 shows that the general trend of the voltage distribution is consistent in three modes. In mode 2, the voltage deviation is minimum because there are 2 ESS units with distributed connection and lower ESS capacity, compared to that for the mode1. Moreover, it is observed that mode 5 has the maximum voltage deviation. This may be attributed to several reasons, as the following: 1)The normalized droop control is adopted by ICs. Therefore, the AC frequency couples with the DC voltage. 2) There is no slack bus in the system. However, the distributed control has low dependency on the communication and the locations of units in the system. In all modes, the frequency and voltage deviations are compensated by the secondary control, which is not discussed in this study.

5.2.2Algorithm Performance in The Operation of The Multi-DC Subgirds IHMG System During The Load Fluctuation

A series of power flows are solved for evaluating the quasi-steady-state behaviors of the system in different operational modes. Firstly, the AC load at the third bus of the AC subgrid increases from 0 to o.6 p.u., then the DC load at the sixth bus of the DC subgrid 1 increases from 0 to 0.3 p.u. It is intended to investigate the influence of the control method of units on the dynamic characteristics of the IHMG during the load fluctuation on a relatively fast time scale.

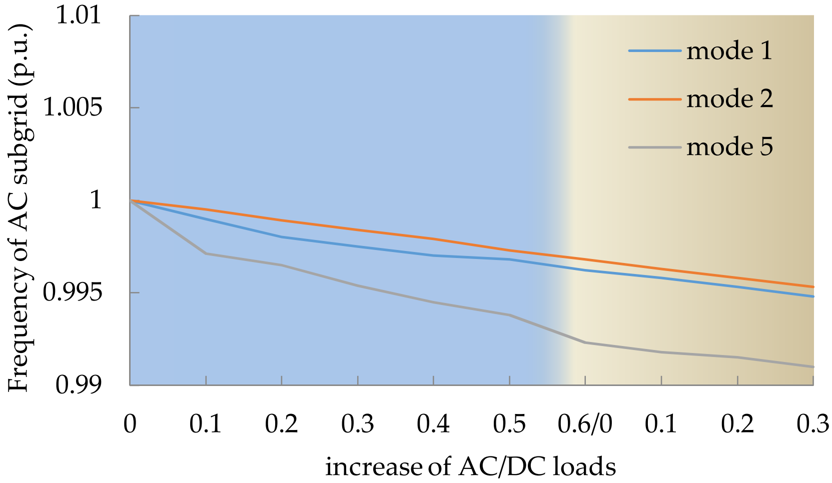

Fig 9. The distribution of the AC frequency of IHMG for the fluctuating AC/DC load

Fig 9 illustrates the frequency evolution of the AC subgrid in different modes during the AC/DC load fluctuation. The AC load fluctuation occurs in the blue region, while the DC fluctuation occurs in the yellow region, subsequently. Fig 9 indicates that the AC frequency is more affected by the load fluctuation in the distributed control mode 5 in comparison to the centralized control modes1 and 2. Because the AC terminal of IC adopts the constant, the AC voltage control operates as a slack bus in AC subgrid in these modes. On the other hand, considering the distributed spatial layout and increasing the number of ESS to 2, although there are the same total capacity in both modes, the frequency has a smaller deviation in mode 2 than the one in the mode 1.

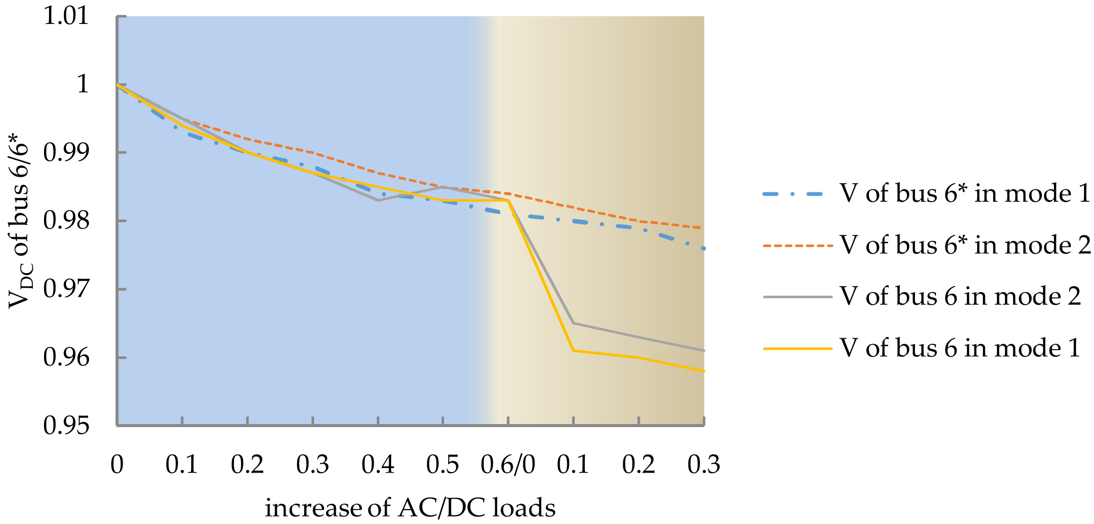

Fig 10. The distribution of the DC voltage of IHMG forthe fluctuating AC/DC load

Fig 10 presents the evolution of the DC voltage of the sixth bus in the DC subgrid 1 and the one of the bus6* in the DC subgrid 2 for modes 1 and 2.It is found that when the AC load fluctuation occurs, the DC terminal of the IC1 and IC2 is controlled in the constant V mode and it operates as the DC slack bus. Therefore, there is a slight drop in the DC voltage amplitude. Fig 10indicates that when the DC load increase, the DC voltage amplitude drops. It is observed that the most serious drop occurs in the sixth bus of the DC subgrid 1, as the point of load fluctuation. In the no load fluctuation area (i.e. DC subgrid 2), there is a slight drop in the DC voltage. Moreover, the ESS units

Preprints (www.preprints.org) | NOT PEER-REVIEWED | Posted: 6 May 2019 doi:10.20944/preprints201905.0067.v1
Peer-reviewed version available at Energies 2019, 12, 2253; doi:10.3390/en12122253

handle power variations of the whole system, whilethe IC unit handles only the power variations in the DC subgrid in modes 1 and 2.

It is found that the suppression of voltage deviation in the mode 2 is better than the one in mode 1.Because the spatial distributed connection of the ESS in mode 2 is better the aggregate connection of the ESS in suppressing power variations.

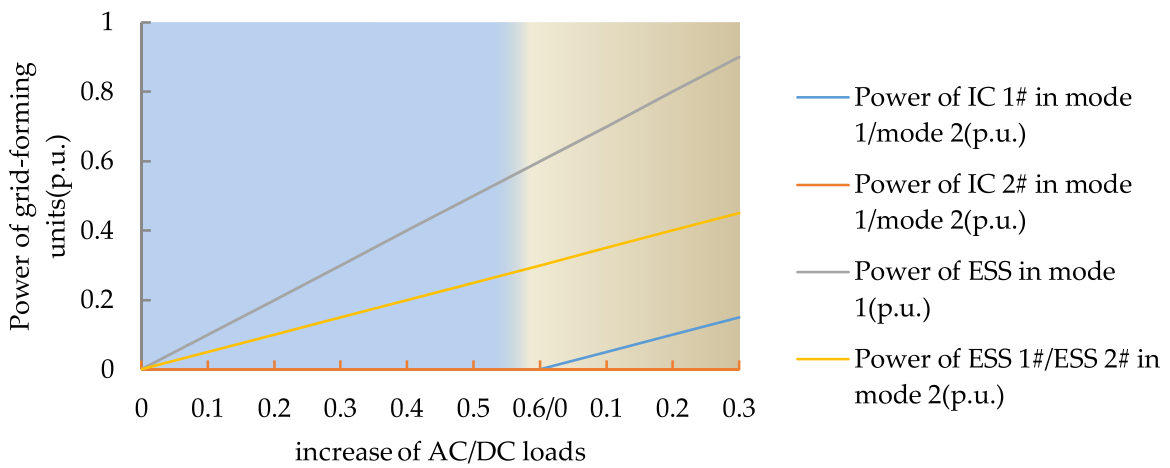

Fig 11. The distribution of the output power of the ESS/IC in IHMG for fluctuation AC/DC load

Fig 11illustrates the variation of ESS/IC's performance in the power handling caused by the load fluctuation in modes 1 and 2. In both modes, the IC1 transfers the same power from the AC to DC subgrid only when the DC load fluctuation occurs. It is found that the IC2 has no power transmission for no DC load fluctuation in the DC subgrid 2.The total output power of the ESS unit is the same in both modes. However, with different spatial configuration, the total output power of the ESS with aggregate connection is averagely allocated of two identical ESS units with the distributed connection. It is concluded that the latter is more effective in suppressing the power variation.

5. Conclusion

ESS and IC units play a decisive role in the frequency and voltage stability of the AC/DC IHMG. In widely applicable hierarchical control architectures, there are various primary control modes adopted by units for maintaining the stable operation of the IHMG. In the present study, a new PF model is proposed for analyzing various operating characteristics of the IHMG system in adopting different primary control methods. The proposed model applies the unified equation and can solve the PF problem for the AC and DC portions of the IHMG, simultaneously. Employing three binary matrices as the input parameter of the unified equation, five operation modes of the IHMG with different primary control strategies and component structures are described, which shows the high degree of flexibility of the proposed PF model. The effectiveness of the new PF model is investigated by comparing the calculated results with the steady-state solution of the MATLAB software.

It is found that for the multiple DC subgrids IHMG, the PF solution enables the use of lower-size energy storage systems and it achieves better effects for suppressing power variations. Therefore, it is concluded that the utilizing the proposed method improves the reliability of the system.

References

1. Wang,P.; Goel, L.; Liu, X.; Ghoo, F.H. Harmonizing AC and DC: A Hybrid AC/DC Future Grid Solution. IEEE Power Energy Mag. 2013,11, [CrossRef].
2. Unamunon,E.; Barrena,J.A. Hybrid ac/dc microgrids—Part I: Review and classification of topologies. Renew. Sustain.Energy Rev.2015,52,1251-1259.
3. Unamunon,E.; Barrena,J.A. Hybrid ac/dc microgrids—Part II: Review and classification of control strategies. Renew. Sustain.Energy Rev.2015,52,1123-1134
4. Hossain, M.A.; Pota, H.P.; Issa, W.; Hossain, M.J. Overview of AC Microgrid Controls withInverter-Interfaced Generations.Energirs,2017,10,1300.
5. Han, Y.; Li, H.; Shen, P.; Coelho, E.A.A.; Guerrero, M. Review of Active and Reactive Power Sharing Strategies in Hierarchical Controlled Microgrids. IEEE Trans. Power Electron. 2017,32,2427-2451
6. Guerrero, J.M.; Chandorkar, M.; Lee, T.L. Advanced Control Architectures for Intelligent Microgrids—Part I: Decentralized and Hierarchical Control. IEEE Trans. Ind. Electron. 2013, 60, 1254-1262.
7. Vandoorn, T.L.; Vasquez, J.C.; Kooning, J.D.; Guerrero, J.M.; Vandevelde, L. Microgrids: Hierarchical Control and an Overview of the Control and Reserve Management Strategies. IEEE Trans. Ind. Electron. 2013, 7, 42-55.
8. Han,Y.; Li, H.; Shen, P.; Coelho, E.A.A.; Guerrero, J.M.Review of Active and Reactive Power Sharing Strategies in Hierarchical Controlled Microgrids. IEEE Trans. Power Electron.2017,32,2427 - 2451.
9. Grainger,J.J.; Stevenson,W.D. Power System Analysis.; McGraw-Hill; New York, 1994.
10. Aprilia, E.; Meng, K.; Hosani, M. A. ; Zeineldin, H.H. Unified Power Flow Algorithm for Standalone AC/DC Hybrid Microgrids. IEEE Trans. Smart Grid 2019,10 ,639 - 649.
11. Eajal,A. A.;Mohamed,A. A.; El-Saadany,E. F.A Unified Approach to the Power Flow Analysisof AC/DC Hybrid Microgrids.IEEETrans. Sustain. Energy 2016, 7, 1145-1158.
12. Hamad.A.A. ; Azzouz,M.A. ; Saadany,E.F.E.A Sequential Power Flow Algorithm for Islanded Hybrid AC/DC Microgrids. IEEE Trans. Power Syst,2016,31, 3961 - 3970
13. Li, C.L.; Chaudhary, S.K.; Savaghebi, M.S.; Vasquez, J.C.; Guerrero, J.M. Power Flow Analysis for Low-Voltage AC and DC Microgrids Considering Droop Control and Virtual Impedance. IEEE Trans. Smart Grid 2017, 8, 2754 - 2764.
14. Hamad, A.A.; Salama, M.M.; EL-Saadany,E.F.; Novel Load Flow Algorithm for Islanded AC/DC Hybrid Microgrids. IEEE Trans. Smart Grid 2019,10, 1553 - 1566.
15. Ahmed, H.M.A.; Eltantawy, A.B.; Salama, M.M.A.; A Generalized Approach to the Load Flow Analysis of AC–DC Hybrid Distribution Systems. IEEE Trans. Power Syst.2017, 2117 - 2127.
16. Aprilia, E.; Meng,K.; Hosani, M.A.; Zeineldin, H.H.; Dong, Z.Y. Unified Power Flow Algorithm for Standalone AC/DC Hybrid Microgrids. IEEE Trans. Smart Grid 2017,10, 639 - 649.
17. Aprilia, E.; Meng, K.; Dong, Z.Y.; Jia, Y.W.; Xu, Z.Hierarchical power flow algorithm for standalone hybrid AC/Multi-DC microgrids.The proceedings of 2017 IEEE Power & Energy Society General Meeting, Chicago, IL , 16-20 July 2017.
18. Nassar, M.E.; Hamad, A.A.; Salama, M.M.; EL-Saadany, E.F.A Novel Load Flow Algorithm for Islanded AC/DC Hybrid Microgrids.IEEE Trans. Smart Grid 2019,10,1553 - 1566.
19. Wang, W.; Barnes, M. Power Flow Algorithms for Multi-Terminal VSC-HVDC With Droop Control. IEEE Trans. Power Syst.2014, 29, 1721 - 1730.
20. Baradar, M.;Ghandhari, M. A Multi-Option Unified Power FlowApproach for Hybrid AC/DC Grids Incorporating Multi-TerminalVSC-HVDC. IEEE Trans. Power Syst., 2013, 28, 2376–2383.
21. Narayanan, K.N.; Mitra, P.A comparative study of a sequential and simultaneous AC-DC power flow algorithms for a multi-terminal VSC-HVDC system. The proceedings of 2013 IEEE Innovative Smart Grid Technologies-Asia ,Bangalore,India, 10-13 Nov. 2013
22. Baradar, M.; Ghandhari, M.; Hertem, D.V.The modeling multi-terminal VSC-HVDC in power flow calculation using unified methodology.The proceedings of 2011 2nd IEEE PES International Conference and Exhibition on Innovative Smart Grid Technologies,Manchester, UK, 5-7 Dec. 2011.

23. Beerten,J.; Cole, S.; Belmans,R. A sequential AC/DC power flow algorithm for networks containing Multi-terminal VSC HVDC systems.IEEE Power and Energy Society General Meeting,Providence, Rhode Island, 25-29 July 2010.
24. Nehrir,M.H. ; Wang,C. ; Strunz,K. ; Aki,H.; Ramakumar,R. ; Bing,J. ; A Review of Hybrid Renewable/Alternative Energy Systems for Electric Power Generation: Configurations, Control, and Applications. IEEE Trans. Sustain. Energy 2011,2, 392 - 403
25. Bouzid, A.B.; Guerrero, J.M.; Cheriti, A.; Bouhamida, M.; Sicard, P.; Benghanem, M.A survey on control of electric power distributed generation systemsfor microgrid applications.Renew. Sustain.Energy Rev. 2015, 44, 751-766.
26. Ahn, S.J.; Park, J.W.; Chung, L.Y.; Moon, S.L.; Kang, S.H.; Nam, S.R.;Power-Sharing Method of Multiple Distributed Generators Considering Control Modes and Configurations of a Microgrid.IEEE Trans. Power Del. 2010, 25, 2007 - 2016.
27. Dragičević,T.;Lu,X.;Vasquez,J.C.;Guerrero,J.M.DC Microgrids—Part I:A Review of Control Strategies and Stabilization Techniques.IEEE Trans. Power Electron. 2016, 31, 4876 - 4891.
28. Palizban,O.; Kauhaniemi, K.; Guerrero, J.M.Microgrids in active network management—Part I: Hierarchical control, energy storage, virtual power plants, and market participation. Renew. Sustain.Energy Rev.2014,36,428-439.
29. Aneke, M.; Wang, M. Energy storage technologies and real life applications–A state of the art review.Appl Ereng.2016,179,350-377.
30. Loh, P.C.; Li, D.; Chai, Y.K.; Blaabjerg, F.Autonomous Operation of Hybrid MicrogridWith AC and DC Subgrids. IEEE Trans. Power Electron.2012,28, 2214 - 2223.
31. Xia,Y.;Peng,Y.G.;Yang,P.C.;Yu,M.;Wei,W.Distributed Coordination Control for Multiple Bidirectional Power Converters in a Hybrid AC/DC Microgrid. IEEE Trans. Power Electron.2017,32,4949 - 4959.
32. Nocedal,J.; Wright, S. J. numerical optimization ,2nd ed.; Springer; New York,2006;pp.66-91.
33. IEEE Guide for Design, Operation,and Integration of Distributed Resource IslandSystems with Electric Power Systems.IEEE Std 1547.4-2011,2011,1 - 54
34. Grainger, J. J.; Stevenson, W. D. Power System Analysis,1st ed.; McGraw-Hill College; New York,1994;pp1-361.
35. Chen, Y. C. ; Dong, P. ; Wu, Z. D. Analysis of power flow in wind farm with matpower.The proceedings of 2017 7th International Conference on Power Electronics Systems and Applications - Smart Mobility, Power Transfer & Security , Hong Kong,China, 12-14 Dec. 2017
36. Zimmerman, R.D.; Daniel, R.; Murillo-Sanchez, C.E.; Thomas, R. J. MATPOWER: Steady-State Operations, Planning, and Analysis Tools for Power Systems Research and Education. IEEE Trans. Power Syst,2011,26, 12 - 19